



PERGAMON

Deep-Sea Research II 49 (2002) 2403–2423

DEEP-SEA RESEARCH
PART II

www.elsevier.com/locate/dsr2

Zooplankton spatial distributions in coastal waters of the northern Arabian Sea, August, 1995

Gary L. Hitchcock^{a,*}, Peter Lane^a, Sharon Smith^a, Jiangan Luo^a,
Peter B. Ortner^b

^a *Division of Marine Biology & Fisheries, Rosenstiel School of Marine and Atmospheric Science, University of Miami,
4600 Rickenbacker Cswy., Miami, FL 33149, USA*

^b *Ocean Chemistry Division, Atlantic Oceanographic and Meteorological Laboratory, NOAA, 4301 Rickenbacker Cswy.,
Miami, FL 33149, USA*

Received 3 April 2001; received in revised form 20 November 2001; accepted 15 December 2001

Abstract

The spatial distribution of zooplankton biomass was surveyed in coastal waters of the northern Arabian Sea during the 1995 Southwest Monsoon (August) on cruise MB 95-06 of the NOAA Ship *Malcolm Baldrige*. Vertical patterns of displacement volumes from a limited set of paired day–night MOCNESS tows suggest there was little diel vertical migration in the coastal waters off the southern Arabian Peninsula. Zooplankton biomass varied from 5.2 to 15.1 g dw m⁻² (178–517 mM C m⁻²) in the upper 200–300 m of Omani coastal waters. Distributions of acoustic backscatter were mapped in eight daytime acoustic Doppler current profiler transects in coastal waters off Oman and Somalia. Several transects contained maxima in acoustic backscatter that coincided with cool, fresh surface features that were several tens of kilometers wide. Although there was considerable scatter in the relationship between acoustically determined biomass (ADB) of zooplankton and surface temperature, there was a trend of increased biomass in the cool surface temperatures of the Omani upwelling zone. Acoustic transects crossed two filaments that extended seaward from upwelling centers off Oman and Somalia. Estimated zooplankton ADB exported from the upwelling zones in the surface features was on the order of 300 kg dw s⁻¹. The physical and biological characteristics of filaments maintain zooplankton associated with upwelling areas, such as *Calanoides carinatus*, as they are advected offshore from coastal upwelling zones. © 2002 Published by Elsevier Science Ltd.

1. Introduction

Knowledge of the spatial scale of zooplankton distributions is essential to understand the mechanisms by which physical and biological processes structure marine ecosystems. The spatial

distributions of zooplankton result from a combination of physical processes, such as advection and diffusion (Mackas et al., 1985), and biological processes, such as diel vertical migration and predation (Folt and Burns, 1999). A large proportion of the variance in zooplankton spatial distributions in coastal waters occurs at the mesoscale (Powell, 1995; Ashjian et al., 2001). Coastal upwelling regions, in particular, have ‘patchy’ zooplankton distributions at scales of

*Corresponding author.

E-mail address: ghitchcock@rsmas.miami.edu
(G.L. Hitchcock).

10–100 km. The spatial variability of zooplankton in coastal upwelling zones reflects complex circulation patterns and biological processes such as diel and ontogenetic migrations (e.g., Verheye et al., 1992).

The surface waters of the northern Arabian Sea are influenced by monsoon winds that produce a strong upwelling response in summer. A low altitude atmospheric feature, the Findlater Jet, begins to develop in early summer along the eastern coast of Africa, and by mid-summer intense, southwesterly winds extend across the entire northern Arabian Sea. This wind regime constitutes the southwest (SW) monsoon (Schott, 1983). During the SW monsoon, large coastal upwelling centers form off Oman (Shi et al., 2000) and Somalia (Smith and Codispoti, 1980) in response to Ekman transport and the vorticity balance, respectively. Upwelling also occurs offshore between the shelf break and the axis of the Findlater Jet in the northern Arabian Sea in response to the curl of the wind stress and other forcing (Lee et al., 2000).

Zooplankton are an important component of pelagic ecosystems in the northern Arabian Sea throughout the year (Smith et al., 1998b; Roman et al., 2000; Baars and Oosterhuis, 1997). One of the major foci of the US Joint Global Ocean Flux Study (US JGOFS) was to understand what role zooplankton have in carbon cycling in the northern Arabian Sea, and how zooplankton respond to monsoon forcing (Smith et al., 1998a). The Arabian Sea Expedition consisted of 17 cruises that repeated a suite of physical, chemical, and biological observations along transects orthogonal to the Omani coastline (Smith et al., 1998a). Several investigators examined zooplankton distributions between September 1994 and December 1995 to define relationships between monsoon processes and zooplankton dynamics. Smith et al. (1998b), Wishner et al. (1998), and Roman et al. (2000) surveyed mesozooplankton biomass distributions with multiple opening/closing nets and environmental sampling systems (MOCNESS) and Bongo nets seaward of the Omani coast to 10°N, 68°E. They found mesozooplankton biomass was highest within several hundred kilometers of the coast, and declined seaward of the axis of the

Findlater Jet. Ashjian et al. (2002) also found higher acoustically derived zooplankton biomass inshore of the Findlater Jet than offshore during the SW monsoon season.

Coastal waters are advected offshore in surface filaments from both the Omani (Manghnani et al., 1998) and Somali (Hitchcock et al., 2000) upwelling zones during the SW monsoon. Filaments that originate near the Omani coast still contain high concentrations of nitrate and chlorophyll *a* several hundred kilometers offshore (Brink et al., 1998; Barber et al., 2001). These features have been recognized as potentially important mechanisms that could export zooplankton from the Omani upwelling zone (Ashjian et al., 2002). Coastal waters with high pigment concentrations also are advected seaward from the Somali upwelling zone in filaments that wrap around the northern edge of a large anticyclonic eddy, the Great Whirl (Smith, 1984; Müller-Karger et al., 1995; Hitchcock et al., 2000). Bakun et al. (1998) hypothesized that zooplankton and larvae may have a limited residence time in the Somali upwelling zone due to rapid offshore export in these filaments.

In August 1995, we surveyed zooplankton distributions in the coastal waters of the northern Arabian Sea on the NOAA Ship *Malcolm Baldrige* (cruise MB-95-06). This cruise, sponsored by the US Global Ocean Ecosystems Dynamics (GLOBEC) Program, began about two weeks before the US JGOFS late SW monsoon cruise, TN050. The main objective of the US GLOBEC Program in the Arabian Sea was to study the population dynamics of higher trophic levels, specifically zooplankton and fish stocks (GLOBEC, 1993). The GLOBEC field study consisted of two cruises on the NOAA Ship *Malcolm Baldrige* that complemented the US JGOFS Program by extending observations south along the Omani coast and to Somalia. The first GLOBEC cruise was in May 1995 during the spring intermonsoon (SI), and the second was in August during the SW monsoon (see Luo et al., 2000).

During the August cruise, the *Baldrige* completed a 1000 km transect along the coast of the southern Arabian Peninsula, and then conducted a brief survey of coastal waters at the outer edge of the Somali upwelling zone (Fig. 1). Baars and

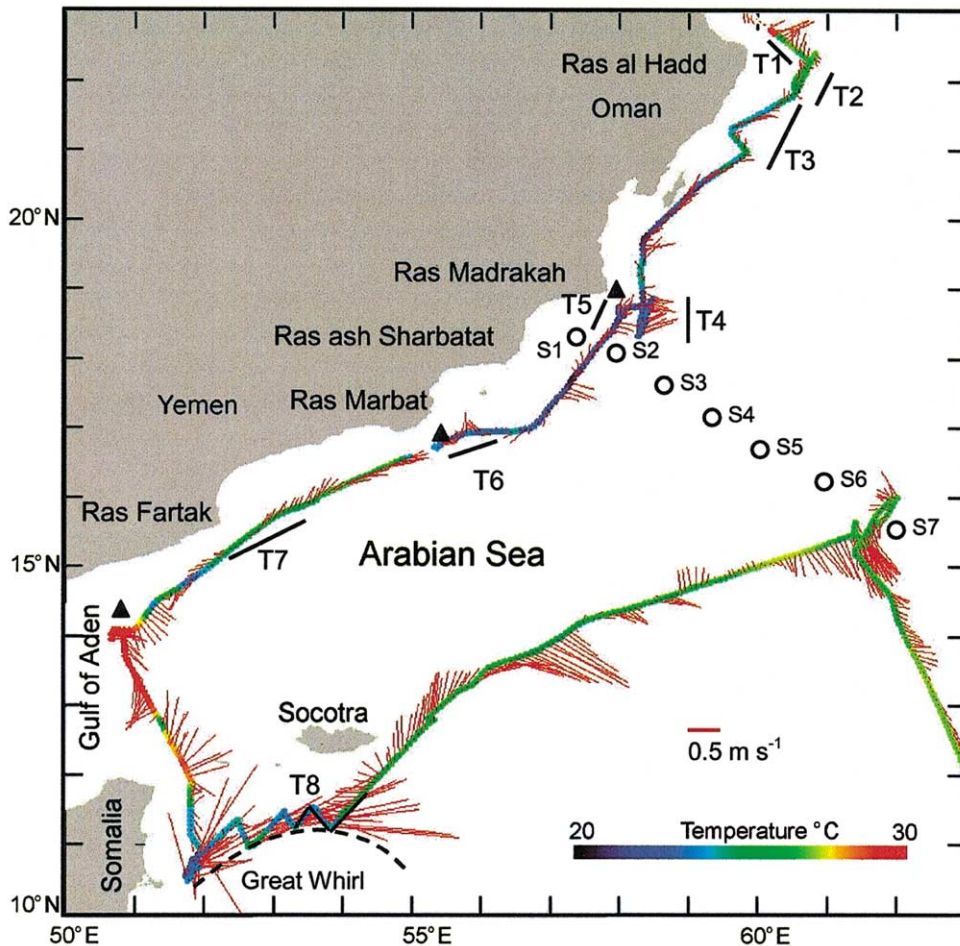


Fig. 1. Cruise track of NOAA Ship *Malcolm Baldrige* in the northern Arabian Sea in August 1995. Surface current vectors, shown in red, are from the upper depth bin (22–30 m) of a hull-mounted ADCP. The positions of the acoustic backscatter transects are designated as T1–T7. (▲) correspond to the position of three paired diurnal-nocturnal MOCNESS tows; M42 and M43 are near T3, M45 and M46 are near T4, and M48 and M49 are west of T5. The (○) indicate the position of stations S2–S7 on the southern US JGOFS line (see Smith et al., 1998a).

Osterhuis (1997) have described zooplankton biomass distributions from 50 to 300 μm mesh ring nets in the Somali coastal waters from MB-95-06. The acoustic signatures associated with diel vertical migration of zooplankton and nekton during this cruise have been analyzed by Luo et al. (2000). They present plots of acoustic backscatter centered at dawn and dusk from the May and August cruises, as well as zooplankton biomass data in four combined day–night MOCNESS tows used to validate the acoustic data.

Additionally, they provide a section of acoustically determined zooplankton biomass along a 1500 km transect in the north central Arabian Sea from the SW monsoon cruise (MB-95-06).

This paper investigates zooplankton distributions in Omani and Somali coastal waters in relation to coastal upwelling zones. The first objective was to determine vertical distributions of zooplankton in Omani coastal waters from MOCNESS tows. Zooplankton biomass from MOCNESS tows are utilized to assess

zooplankton biomass in the Omani upwelling zone relative to that measured further offshore on US JGOFS cruise TN050. Based on observations from other coastal upwelling systems (Boyd and Smith, 1983; Smith, 1992), where ‘classical’ diatom-copepod-fish food webs predominate, we hypothesized that highest zooplankton biomass would be seaward of the upwelling zone. Next, we characterize the spatial distribution of zooplankton in Omani coastal waters from acoustic backscatter to determine the spatial scales of variability. Finally, we estimate zooplankton transport in filaments that originate at the edge of the Omani and Somali upwelling zones to assess potential export of zooplankton from regions of intense seasonal upwelling.

2. Methods

2.1. Cruise overview

The SW monsoon GLOBEC cruise of the *Malcolm Baldrige* departed from Muscat, Oman on July 31, 1995. The ship headed south, parallel to the Omani coast, recording acoustic data and surface properties (Fig. 1), and reached Cape Fartak, Yemen (14.5°N, 53°E) on August 9. Throughout the cruise, acoustic surveys were interspersed with net tows for zooplankton using a 1 m² (MOCNESS; Wiebe et al., 1976) with 153 µm mesh nets (MOC01), and net tows for small fish with a 10 m² MOCNESS with 3 mm mesh nets (MOC10). Locations of three paired day–night MOCNESS tows are designated in Fig. 1 near Ras Madrakah, Ras Marbat, and Ras Fartak. On August 10, the cruise proceeded south across the eastern Gulf of Aden and reached the Somali upwelling zone on August 11. The ship was unable to secure diplomatic clearance to enter Somali territorial waters, and therefore, we did not survey the interior of the upwelling zone. On August 12 and 13, a series of MOCNESS tows were attempted at the eastern edge of the upwelling zone (10.5°N, 52.0°E). Unfortunately, fast surface currents (>2 m s⁻¹; Hitchcock et al., 2000), high vertical current shear, and high winds resulted in tangled nets in all MOCNESS tows

taken in Somali waters. The tows therefore undersampled zooplankton biomass. Additionally, zooplankton were difficult, or impossible, to identify since they were mutilated in the tangled nets.

On the afternoon of August 13, the ship headed east to conduct repeated crossings of a cool surface filament that extended east from the upwelling zone and encircled the northern perimeter of the Great Whirl (Hitchcock et al., 2000). Late on August 14 the ship headed NE toward a mooring array maintained by the Office of Naval Research’s (ONR) Forced Upper Ocean Dynamics Program at 15.5°N, 61.5°E (Fig. 1). Following two days of net tows at the mooring array, the ship went southeast to arrive at Diego Garcia on August 21, 1995.

2.2. Surface properties

Surface property distributions were mapped with a Seabird thermosalinograph recording temperature and conductivity from an intake line on the bow at 3 m depth. Conductivity and temperature data were logged concurrently with position from a Global Positioning System receiver. Chlorophyll *a* fluorescence was recorded in the surface seawater by a Turner Designs Model 10 fluorometer. The flow-through fluorometer data were calibrated with filtered pigment samples (Hitchcock et al., 2000). Total chlorophyll *a* concentration (sum of chlorophyll *a* and phaeopigment *a*) was plotted as a function of the corresponding fluorescence value (FL) from the flow-through fluorometer for samples collected during the daytime transects. This yields a linear regression of the form

$$\text{'total' chlorophyll } a = (4.6235 \times \text{FL}) - 0.88, \quad (1)$$

where FL is fluorescence ($r^2 = 0.90$).

2.3. Zooplankton sampling

A 1 m² MOCNESS collected zooplankton in stratified tows through the upper 1000–1200 m with nine 153 µm mesh nets at six stations (Table 1). The first tow interval (net 1) was from the surface to the deepest depth, then eight depth

Table 1
Location of daytime ADCP transects and MOCNESS tows from *Baldrige* cruise MB95-06

Date	Event	Region	Location	Temperature (°C)
Aug. 1	Transect 1	Ras al Hadd (E)	Start: 22.56°N, 60.41°E End: 22.16°N, 60.71°E	26.5–27.1
Aug. 2	Transect 2	Ras al Hadd (E)	Start: 21.78°N, 60.54°E End: 22.25°N, 60.74°E	25.0–26.9
Aug. 3	Transect 3	Ras al Hadd (SE)	Start: 21.80°N, 60.53°E End: 20.74°N, 59.51°E	23.6–26.1
Aug. 4	Transect 4	Ras al Madrasah	Start: 18.83°N, 58.34°E End: 18.79°N, 58.44°E	21.4–23.2
Aug. 5	Transect 5	Ras al Madrasah	Start: 18.65°N, 58.00°E End: 18.43°N, 57.92°E	21.4–21.9
Aug. 5	MOC43	Ras al Madrasah	Day: 18.72°N, 57.99°E	
	MOC42	Ras al Madrasah	Night: 18.73°N, 57.99°E	
Aug. 6	Transect 6	Ras Marbat	Start: 16.96°N, 56.97°E End: 16.72°N, 55.33°E	21.6–23.8
Aug. 7	MOC46	Ras Marbat	Day: 16.77°N, 55.43°E	
	MOC45	Ras Marbat	Night: 16.77°N, 55.47°E	
Aug. 8	Transect 7	Ras Fartak	Start: 15.84°N, 53.30°E End: 14.88°N, 51.91°E	24.0–26.2
Aug. 9	MOC49	Ras Fartak	Day: 14.08°N, 50.69°E	
	MOC48	Ras Fartak	Night: 14.08°N, 50.67°E	
Aug. 14	Transect 8	Somalia	Start: 11.26°N, 53.33°E End: 12.43°N, 54.94°E	22.7–26.1

MOCNESS tows are designated as daytime (Day) or night-time (Night) with the start position. Surface temperatures are provided for the duration of acoustic backscatter transects.

intervals were sampled as the MOCNESS was raised to the surface. Collections in the upper 200–300 m were typically at depth intervals of 50–100 m. The material in the cod end was preserved with formalin and returned to NOAA's Atlantic Oceanographic and Meteorology Laboratory, Miami, FL, USA, for displacement volume measurements (Ahlstrom and Thraikill, 1963). Conversions from displacement volume to dry weight are based on the regressions of Wiebe (1988), with dry weight converted to carbon equivalents through the relationship of Ikeda (1974) (see Smith et al., 1998b). Taxonomic analyses of selected samples were carried out at the Institute for Biology of the Southern Seas (IBSS) in Sevastopol, Ukraine (see Smith et al., 1998b). Although the number of MOCNESS tows was limited, and replicate sampling could not be done due to constraints in the cruise schedule, the observations from MOCNESS tows provide a direct measure of biomass and a description of zooplankton taxa.

Our primary method for assessing zooplankton spatial distributions relied upon acoustic backscatter intensity from a 153-kHz RDI acoustic Doppler current profiler (ADCP) used during daytime. Spatial distributions of zooplankton have been studied by means of acoustic backscatter in a variety of coastal and oceanic regions (Flagg and Smith, 1989; Smith et al., 1992; Heywood, 1996; Zhou et al., 1994; Coyle et al., 1998; Ashjian et al., 2002). In single frequency instruments such as the ADCP, changes in the size or abundance of small zooplankton can yield similar responses (Holliday and Pieper, 1995). Additionally, different morphologies and reflectivity of various taxonomic groups of zooplankton also confound relationships between biomass and echo strength (Stanton et al., 1994); thus, individual calibrations are required in each environment.

Luo et al. (2000) describe the calibration procedure for deriving acoustically determined biomass (ADB) of zooplankton with the ADCP on the *Malcolm Baldrige* with separate regression

equations for the SI and SW monsoons. An objective of Luo et al. (2000) was to evaluate the effect of diurnal vertical migration of larger organisms on the acoustic backscatter intensity from the 153 kHz ADCP. Through concurrent sampling with a 12 kHz transducer, they showed that acoustic backscatter from the ADCP at night was strongly influenced by the presence of large organisms that undergo diel vertical migrations. In the northern Arabian Sea, the diel vertical migration of small nekton, principally myctophids (Gjøsaeter, 1984), and crustaceans (van Couwelaar et al., 1997) result in a strong diel periodicity in the acoustic backscatter in the ADCP (Luo et al., 2000; Ashjian et al., 2002). Since the vertical migration of nekton strongly bias ADCP returns between dusk and dawn, we only consider daytime ADCP observations between 07:00 and 17:00 local time to assess zooplankton spatial distributions.

Acoustic data were collected every 10 s, with averages recorded at 5 min intervals, from the ADCP mounted in the ship's hull at a depth of 6 m. Sampling bins were set at 8 m intervals with the first bin at 22–30 m below the surface. The raw acoustic returns were processed by the Common Data Access System (CODAS version 3.1) developed by Firing et al. (1995). The relationship between acoustic backscatter intensity and meso-zooplankton biomass during the SW monsoon was derived from 35 MOC1 samples matched in space and time with backscatter intensity from the ADCP. For the SW monsoon cruise, the data describe a linear regression of the form

$$\ln \text{biomass (mg dw m}^{-3}\text{)} = 20.51 \text{ (dB)} + 0.2376, \quad (2)$$

where dB is the average backscatter intensity in the corresponding depth bin from the ADCP ($r^2 = 0.52$; $n = 35$; Luo et al., 2000).

The ADB of zooplankton ($\text{g dry weight m}^{-2}$) was estimated from ADCP data from depth bins between 20 and 120 m. This depth interval was chosen to correspond to Ashjian et al. (2002), who surveyed zooplankton distributions with an RDI ADCP on the R.V. *Thomas G. Thompson*. The ADB for the *Baldrige* transects was derived for each depth bin with Eq. (2), using an upper limit of -62 dB to limit sampling bias from large organisms (e.g., Coyle et al., 1998). The 5 min ADB

average in each depth bin was multiplied by the depth interval (8 m), and the total ADB summed from successive bins between 22 and 120 m. The depth-integrated ADB was plotted as a function of surface temperature measured at the ADCP sensing head to determine if cooler surface temperatures correspond to higher zooplankton biomass.

We utilized zooplankton ADB on two transects to estimate the horizontal offshore flux of zooplankton in filaments. These filaments were located at the eastern edge of coastal upwelling zones off Ras Madrasah, Oman and Ras Hafun, Somalia. Transect 4 crossed the filament off Ras Madrasah twice on August 4, while Transect 8 crossed a cool filament east of the Ras Hafun upwelling zone on August 14 (Table 1). Estimates of the offshore flux of zooplankton biomass in filaments were made by first extrapolating the location of the individual ADCP profiles (made at 5 min intervals) to a line orthogonal to the surface flow. In both filaments the offshore flow component was to the east. The ADB in each 8 m depth bin (mg dw m^{-2}) was averaged for successive profiles, as was the corresponding offshore velocity (m s^{-1}). The two values were multiplied, and the product multiplied by the station spacing (kilometers). The offshore flux of ADB was then summed from the individual depth bins in intervals between the successive profiles to yield an offshore flux in terms of kg dw s^{-1} .

3. Results

3.1. Zooplankton biomass and vertical distributions in MOCNESS samples

Estimates of zooplankton biomass from MOCNESS tows are expressed as both dry weight and carbon to provide comparisons with the carbon-based values used in all US JGOFS studies (Table 2). Since sampling depths differed among stations, the depth-integrated biomass also was normalized to a unit volume (m^{-3}) for the comparisons. Zooplankton biomass in MOCNESS tows from coastal waters of the southern Arabian Peninsula varied 3-fold, from 5.2 to

Table 2

Zooplankton biomass estimated from displacement volume on GLOBEC (NOAA Ship *Baldrige*) and US JGOFS (R.V. *Thomas G. Thompson*) cruises during the Southwest Monsoon, 1995

Station	Net tow	Interval (m)	Zooplankton biomass			
			Integrated (m^{-2})		Unit volume (m^{-3})	
			(mg dw)	(mM C)	(mg dw)	(mM C)
GLOBEC						
M42	MOC (N)	0–200	5210	178	26.1	0.89
M43	MOC (D)	0–200	7258	248	36.3	1.24
M45	MOC (N)	0–300	15,132	517	50.4	1.72
M46	MOC (D)	0–300	8342	285	27.8	0.95
M48	MOC (N)	0–300	9776	334	32.6	1.11
M49	MOC (D)	0–300	6498	222	21.7	0.74
US JGOFS						
S1	Bongo (D)	0–50	10,302	352	118.2	7.04
S2	MOC (D)	0–300	12,059	412	40.1	1.37
	MOC (N)	0–300	12,117	414	40.1	1.38
S3	Bongo (N)	0–200	9161	313	45.7	1.56
S4	MOC (D)	0–300	17,707	605	58.8	2.01
	MOC (N)	0–300	13,112	448	43.6	1.49
S7	MOC (D)	0–300	3600	123	12.0	0.41
	MOC (N)	0–300	6380	218	21.1	0.72

Positions of GLOBEC stations are given in Table 1. Data from US JGOFS stations S1 to S7 are from Lane and Smith (1997). Net tows are identified as MOCNESS (MOC) or Bongo tows during the day (D) or night (N).

15.1 g dw m^{-2} . The range in biomass from MOCNESS tows was comparable to that observed in zooplankton ADB, as discussed in Section 3.2. Zooplankton biomasses from MOCNESS tows in the upwelling region off Ras Madrakah and Ras Marbat did not exceed those found at Ras Fartak.

The vertical distribution of zooplankton from six day–night paired tows show the major fraction of zooplankton biomass was in the upper 200 m (Fig. 2), as both day and night tows contained 78–95% of total zooplankton biomass in the upper 200 m. Average concentrations per unit volume (m^{-3}) in the upper 200–300 m varied from 0.74 to 1.72 mM C m^{-2} , or $21\text{--}50 \text{ mg dw m}^{-3}$ (Table 2). Below 300 m, zooplankton biomass was generally $<0.1 \text{ mM C m}^{-3}$ ($<5 \text{ mg dw m}^{-3}$). Although the maximum sampling depth varied from 1000 to 1200 m, there was little contribution to the total water column in the 1000–1200 m depth interval (Fig. 2).

However, differences occurred in day–night biomass distributions within the upper 50 m of

the water column. In the coastal upwelling zone at Ras Madrakah, maximum zooplankton biomass occurred in the upper 50 m during the day (Fig. 2a). The low biomass concentration in the night tow (M42) may have resulted, in part, from under-sampling due to a tangled net in the 50–100 m depth interval (asterisk, Fig. 2a). The daytime tow (M43) provides information on the zooplankton community that can be compared to communities in daytime tows at Ras Marbat and Ras Fartak. The dominant mesozooplankton at Ras Madrakah were primarily *Euphausia furcilia* (11 ind. m^{-3}) which were more abundant at Ras Madrakah than at Ras Marbat in the daytime (5 ind. m^{-3}). Copepod abundance in the upper 50 m at Ras Madrakah was 1600 ind. m^{-3} , similar to the total daytime copepod abundance in the upper 50 m at Ras Marbat. However, at Ras Madrakah the copepodite and adult stages of the copepod *Calanoides carinatus* comprised ca. 50% of all copepods. This is a striking contrast to the copepod community at Ras Marbat and Ras

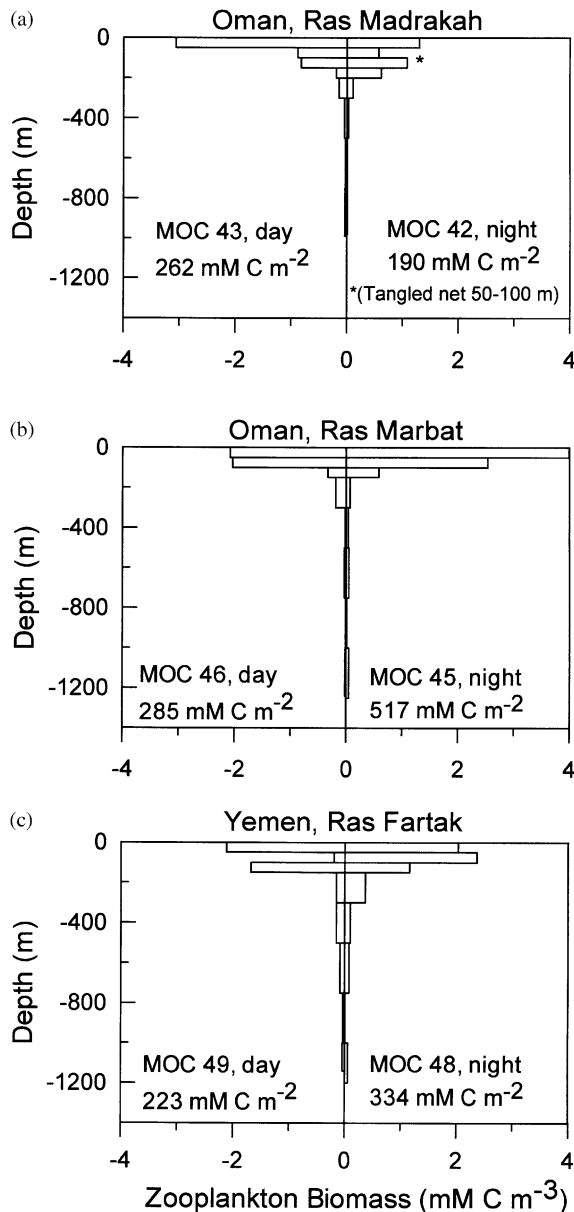


Fig. 2. The vertical distribution of zooplankton biomass as mM C m^{-3} over depth intervals as estimated from displacement volume in paired diurnal–nocturnal MOCNESS tows. Night-time collections are on the right and daytime collections are on the left. The top panel (a) is from paired tows at Ras Madrakah, Oman (M42 and M43), the middle panel (b) is from Ras Marbat, Oman (M45 and M46), and the lower panel (c) is from Ras Fartak, Yemen (M48 and M49). The depth-integrated biomass, as mM C m^{-2} , is given for the depth intervals listed in Table 2.

Fartak where *C. carinatus* comprised only 1% and 0.1% of total copepods, respectively. This species does not undergo diel vertical migration, but completes a seasonal, ontogenetic migration in the upwelling zones (Smith et al., 1998b). Its presence in the cooler surface waters at Ras Madrakah is consistent with its distribution in other upwelling zones of the northern Arabian Sea.

Off Ras Marbat, near the southern limit of the upwelling zone, and at Ras Fartak, the highest zooplankton biomass was observed at night (Fig. 2b and c). The relatively high nocturnal zooplankton biomass at Ras Marbat (M45; Fig. 2b) may partially reflect a diel vertical migration of zooplankton, primarily euphausiids. In M45 the mesozooplankton were dominated by *Euphausia sibogae* (51 ind. m^{-3}) ranging in length from 4 to 11 mm. In the corresponding daytime tow (M46; Fig. 2b), euphausiids were comprised mainly of unidentified furcilia (ca. 5 ind. m^{-3}) < 3 mm in length. The difference in the euphausiid abundance may result from diel vertical migration of larger euphausiids (e.g., Watkins et al., 1985; Barange, 1990; Nordhausen, 1994) or, alternatively, from net avoidance during the day by larger, faster swimming individuals (e.g., Wiebe et al., 1982; Smith, 1991).

The higher zooplankton biomass in the upper 50 m at night off Ras Marbat could be attributed to increased copepod abundance (6700 ind. m^{-3}) compared to daytime abundance (1600 ind. m^{-3}). However, the dominant taxa at Ras Marbat were small-bodied copepods such as *Acartia* spp., *Corycaeus* spp., *Oncaea* spp. and *Paracalanus* spp. in both daytime and night-time tows. Since these genera are not strong vertical migrators, the diel vertical migration of copepods cannot totally account for higher night-time biomass. Night-time abundance of pteropods (154 ind. m^{-3}) and chaetognaths (139 ind. m^{-3}) greatly exceeded daytime abundances, thereby contributing to the increased night-time biomass in the upper 50 m.

At Ras Fartak, in contrast, zooplankton biomass in the upper 50 m was similar in day and night tows (Fig. 2c). Species composition differed from that at Ras Marbat, with *Stylocheiron* spp. furcilia (ca. 8 ind. m^{-3}), *Euphausia sibogae*

(ca. 1 ind. m^{-3}), and several other euphausiid species, each $< 0.5 \text{ ind. m}^{-3}$, dominating biomass in the upper 50 m at night (M48; Fig. 2c). In the daytime tow (M49; Fig. 2c), mesozooplankton in this depth interval were dominated by mastigopus *Sergestes* (post-larval shrimp) at densities of 24 ind. m^{-3} , ranging in length from 4 to 6 mm. Total copepod abundance in the upper 50 m was 1100 ind. m^{-3} at night and 800 ind. m^{-3} during the day. Copepods were dominated by *Paracalanus* spp. in both the day and night tows. Other zooplankton included small (1–4 mm) doliolids (55 ind. m^{-3} during night versus 11 ind. m^{-3} during daytime) and chaetognaths (29 ind. m^{-3} at night versus 41 ind. m^{-3} during daytime).

Zooplankton biomass at Ras Fartak also differed between the day and night in the 50–100 m depth interval (Fig. 2c). Mesozooplankton abundance was low in both day and night tows, and consisted primarily of *Euphausia* furcilia and *Stylocheiron affini*. Copepod abundances were also low (500 ind. m^{-3} at night and 60 ind. m^{-3} during the day) relative to Ras Madrasah and Ras Marbat, and dominated by the small-bodied *Oncaea* spp. Thus, copepod abundance may have partially accounted for the biomass differences observed between day and night tows at Ras

Fartak. The large diel variation in biomass is more likely due to the presence of doliolids, which were 60-fold more abundant at night than at day (ca. 600 ind. m^{-3} in M48 versus 10 ind. m^{-3} in M49).

3.2. Zooplankton ADB in Omani coastal waters

Zooplankton ADB in daytime transects between Ras al Hadd and Ras Fartak showed considerable scatter at SSTs of $21.5\text{--}27^\circ\text{C}$ (Fig. 3a). The data correspond to 807 estimates of zooplankton ADB in seven transects (see Table 1). In general, lower zooplankton biomass occurred at surface temperatures $> 26^\circ\text{C}$, while higher zooplankton biomass occurred at surface temperatures $< 24^\circ\text{C}$. A cluster of relatively low zooplankton ADB at SST of $26\text{--}27^\circ\text{C}$ (mean = 6.8 g dw m^{-2}) correspond to Transects T1 and T2 that were east and south of Ras al Hadd, respectively. Transects T1 and T2 sampled surface waters north of a Jet-frontal system that separates warmer surface waters of the Gulf of Oman from cooler surface waters that upwell along the southern Arabian Peninsula (Böhm et al., 1999).

Perhaps the most striking features in the zooplankton ADB-temperature plot are biomass maxima that occurred in Transects 3, 4, and 8

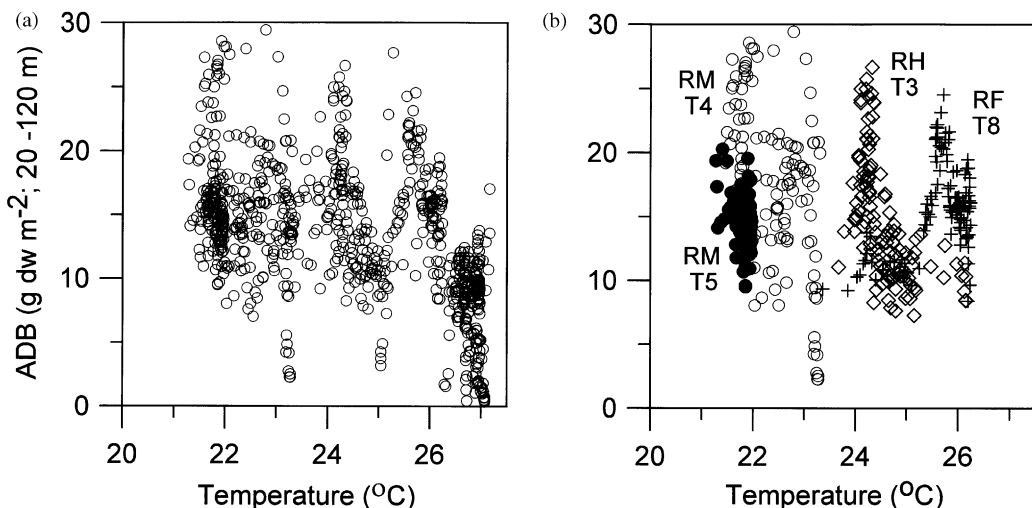


Fig. 3. (a) Acoustically determined biomass (ADB) for zooplankton in Omani coastal waters as a function of surface temperature. The data correspond to the 20–120 m depth interval in Transects T1–T7 (Table 1) (b) As in (a) for Transects T3 (Ras al Hadd (\diamond), T4 (\circ) and T5 (Ras Madrasah (\bullet), and T7 (Ras Fartak ($+$)).

(Fig. 3b). The maximum in zooplankton ADB between 22°C and 23°C was in Transect 4 at the eastern edge of the coastal upwelling zone off Ras Madrakah (T4, RM in Fig. 3b). A maximum in ADB at 24°C was from Transect 3 south of Ras al Hadd (T3, RH in Fig. 3b), while the maximum at 25°C was in warmer surface waters south of Ras Fartak, Yemen (RF, T8 in Fig. 3b). Mean ADB from these three transects varied from 14.7 to 17.1 g dw m⁻², while individual acoustic profiles yielded ADB that ranged from <10 to >25 g dw m⁻². This large scatter contrasts with the limited ADB of 10–20 g dw m⁻² in Transect 5, where the mean zooplankton ADB was 14.9 g dw m⁻² (Fig. 3b). Data in Transect 5 represent zooplankton ADB in the cool, recently upwelled waters near Ras Madrakah. Since the zooplankton-temperature relationships in Transects 3–5, and 8 are distinct, we examined acoustic backscatter in Transects T3–T8, with corresponding surface properties, to determine if the maxima in backscatter coincide with identifiable physical features.

3.3. Acoustic backscatter in Transects T3–T7

Surface physical properties and acoustic backscatter in Transects T3–T7 illustrate that considerable spatial variability exists over tens of kilometers in the coastal waters off the southern Arabian Peninsula. In Transect 3 southeast of Ras al Hadd, for example, maximum acoustic backscatter in the upper 120 m coincided with decreased SST (Fig. 4). A 50 km interval designated by arrows in Fig. 4 corresponds to a region of enhanced backscatter (–70 db to –65 db) and lower SST (<25°C). Surface salinity varied from 35.9 to 36.1 across the width of the region of highest backscatter, with surface chlorophyll *a* concentrations of 0.5–0.7 mg m⁻³. At the southern edge of T3, surface chlorophyll *a* concentrations increased from <1 µg l⁻¹ to >2 µg l⁻¹ as temperature increased to >25°C and surface salinity to >36.2. The gradient in surface properties at the southern end of T3 likely corresponds to a surface front. Surface current vectors from the ADCP, however, suggest relatively weak surface flow across the length of T3 with no divergence or

convergence associated with the thermal front at the southern end of the Transect (Fig. 1).

A transect along the outer margin of the coastal upwelling zone off Ras Madrakah displayed similar coherence between low SST and enhanced acoustic backscatter. Transect T4 was located at the eastern edge of the Ras Madrakah upwelling center (Fig. 1). As the ship steamed south, it crossed a 60 km-wide region where SST was <23°C. At the southern end of this section, SST increased to 23°C, and the ship turned north to repeat the section. The low-temperature sections in T4 are designated with arrows in Fig. 5 with the ship's heading. The surface ADCP vectors and low SST indicate this cool surface feature corresponds to one of the filaments that flowed east from the upwelling zone during the SW monsoon (Brink et al., 1998; Manghnani et al., 1998). The ADCP current vectors at 22–30 m indicate an offshore flow at >1 ms⁻¹, where surface waters were <23°C (Fig. 1). During the repeated crossings of the feature, the highest acoustic backscatter was in the upper 100 m (Fig. 5, top panel). Maximum ADB occurred near the northern end of the two sections where surface temperatures were 22–23.5°C (compare Figs. 3b and 5). Surface temperatures and salinities were 'patchy' within the feature, as temperature varied from 21.5°C to 23°C and salinity from 36.0 to 35.6. Surface chlorophyll *a* concentrations were also variable, ranging from ca. 0.5 mg m⁻³ in the feature to >1.0 mg m⁻³ at the northern edge (Fig. 5). Estimates of total ADB transport within the two successive sections across the feature were similar, at 310 and 294 kg dw s⁻².

On the following day, surface properties and acoustic backscatter were mapped in the coastal upwelling zone in Transect 5 (Table 1, Fig. 1). This 50 km-long transect was parallel to, and ~35 km west of, Transect 4. Near-surface current vectors on T5 were easterly, as in T4, but at maximum velocities of <0.5 ms⁻¹. The acoustic backscatter section shows relatively uniform distribution with depth. Highest backscatter intensity was in the upper 50 m (top panel, Fig. 6). This uniform distribution explains the limited range in ADB in T5, compared to the greater range seen in T3, T4 or T7 (Fig. 3b). Near-surface physical properties

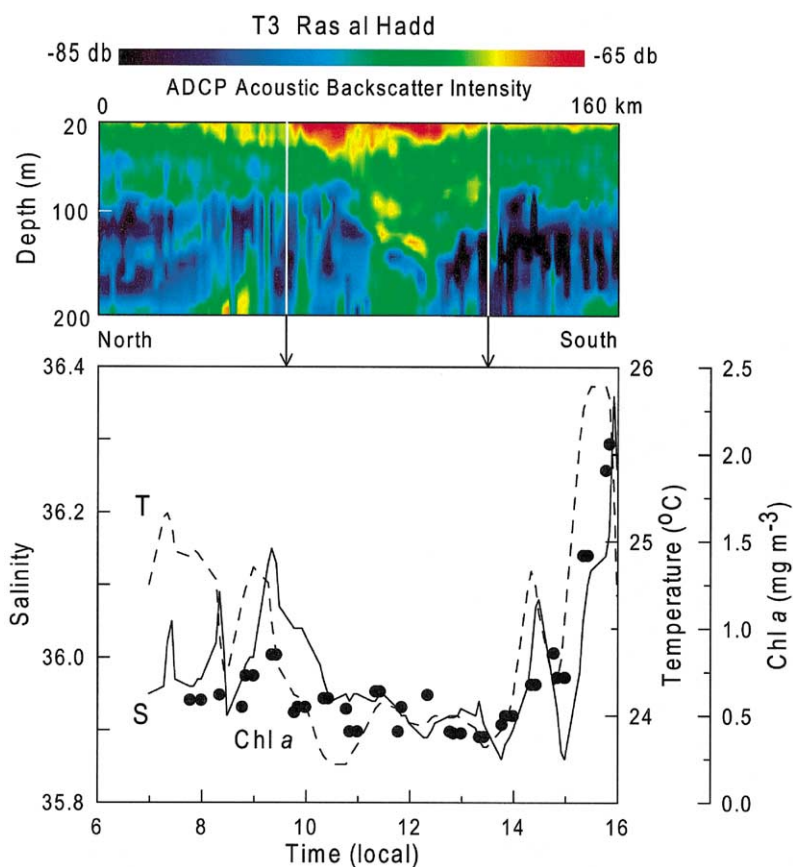


Fig. 4. Upper panel: spatial distribution of acoustic backscatter intensity in the upper 20–200 m along transect T3 in coastal waters southeast of Ras al Hadd, Oman. The upper color bar represents the range in volume backscatter intensity from -85 to -55 dB. Arrows in the ADCP backscatter plot show that maximum acoustic backscatter intensity corresponds to relatively cool fresh surface waters. Lower panel: corresponding surface salinity (—), temperature (---), and total chlorophyll *a* (Chl *a* (●)) from the bow water intake at 3 m. Total chlorophyll *a* concentrations are extrapolated from *in vivo* fluorescence measurements regressed against the sum of chlorophyll *a* + phaeopigment *a* concentrations (see Methods section).

were relatively constant along T5, as SST (21.0 – 21.5°C) and surface salinities (35.65 – 35.70) exhibited less variability than in T4 (compare Figs. 5 and 6). The surface temperature and salinity values recorded on T5 were similar to the minimum found in the upwelling zone during the SW monsoon during the 1963 International Indian Ocean Expedition (Currie, 1992), and the 1995 Arabian Sea Expedition (Morrison et al., 1998). Surface total chlorophyll *a* concentrations varied from 0.6 to 0.8 mg m^{-3} over much of Transect 5, but increased at the southern end to $>1.0\text{ mg m}^{-3}$ as SST decreased. In general, the near-surface

physical properties and plankton distributions suggest there was little spatial variability in the coastal upwelling zone.

The southern extent of the coastal upwelling zone was near Ras Marbat where SST varied from 22°C to 24°C (Fig. 1). Transect 6 spanned 130 km in the surface waters at the southern end of the coastal upwelling zone (Fig. 7). Surface current vectors indicate a northerly, onshore flow in the northern half of T6, and a weak offshore flow in the southern half (Fig. 1). The acoustic backscatter section reveals little structure within the upper 120 m where SST was $>23^{\circ}\text{C}$. In the southern half

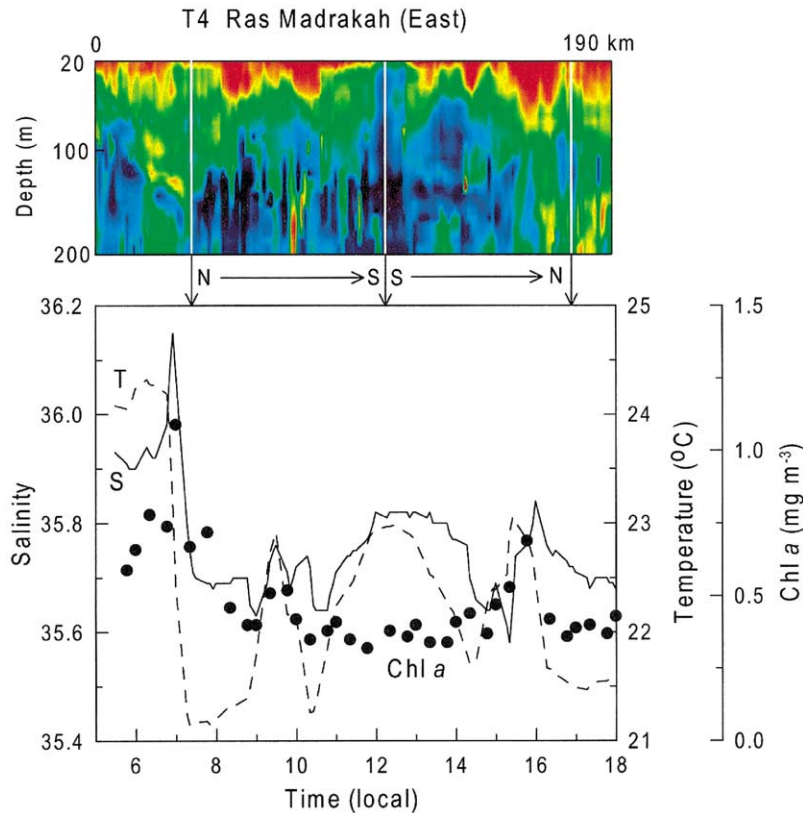


Fig. 5. Upper panel: the spatial distribution of acoustic backscatter intensity in the upper 20–200 m in Transect T4 in coastal waters east of Ras Madrasah, Oman. Color scale as in Fig. 3. Arrows in the ADCP backscatter plot indicate that the maximum acoustic backscatter corresponds to relatively cool fresh surface waters. Lower panel: corresponding surface salinity, temperature, and total chlorophyll *a* (Chl *a*) from the bow water intake at 3 m.

of the transect, south of 16.9°N, 55.7°E (13:00 local time), the SST and surface salinity decreased to ~22°C and 35.6, respectively. Surface chlorophyll *a* concentrations increased from <1 to 8 mg m⁻³ as the ship passed into cooler surface waters. The gradient in surface properties coincides with the position where surface currents changed direction from an onshore to offshore flow (see Fig. 1, T6). South of the surface front, acoustic backscatter was elevated at depths >150 m. This increase in acoustic backscatter was not apparent in the 20–120 m ADB estimates in Fig. 3. The distribution of surface properties, near-surface current vectors, and acoustic backscatter all suggest that a surface front separated two distinct surface regimes at the southern end of the coastal upwelling zone.

The southernmost transect off the southern Arabian Peninsula, Transect 7, was south of Ras Fartak, Yemen. As in Transects at Ras al Hadd (T3) and Ras Marbat (T6), Transect 7 contained SST evidence of a front with an associated maximum in acoustic backscatter. In the northern half of T7, SST was >25°C and chlorophyll *a* concentrations were 1–2 mg m⁻³ (Fig. 8). As the ship crossed the front, SST decreased to <24°C and chlorophyll *a* increased to >2 mg m⁻³. Surface salinities, in contrast, varied over a limited range at 35.85–36.0 along the length of the Transect. As in T6, surface currents in T7 changed direction near the front. North of the front the near-surface currents were to the NE, while south of the front currents flowed to the west (Fig. 1). The maximum ADB in T7 was 20–25 g dw m⁻²

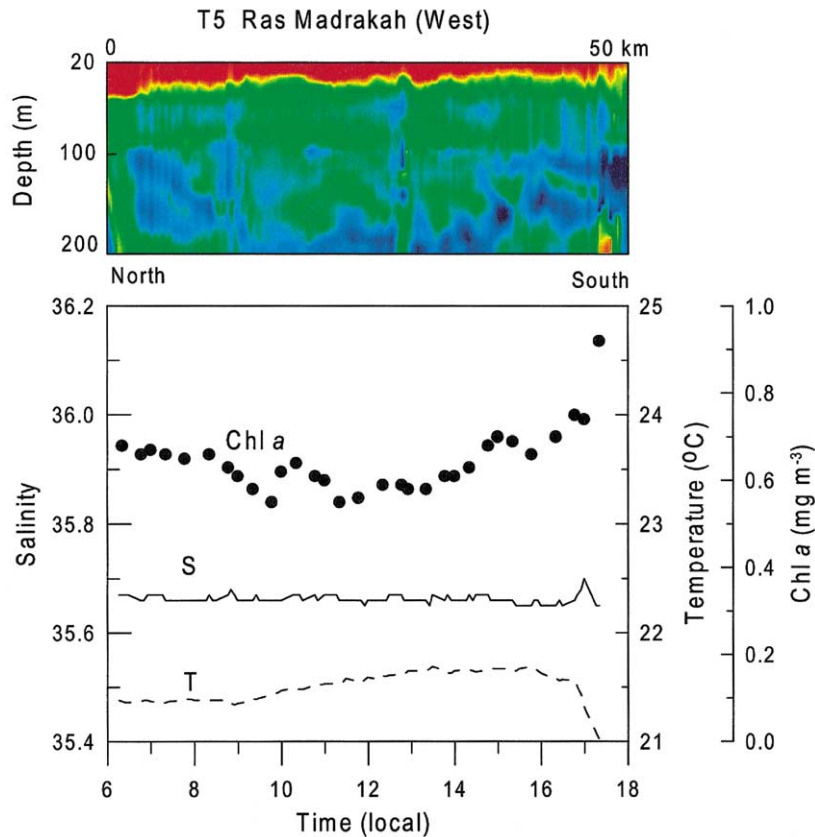


Fig. 6. Upper panel: the spatial distribution of acoustic backscatter intensity in the upper 20–200 m in Transect T5 in recently upwelled waters near Ras Madrakah, Oman. Color scale as in Fig. 3. Lower panel: corresponding surface salinity, temperature, and total chlorophyll *a* (Chl *a*) from the bow water intake at 3 m.

where surface temperatures were 25.5°C (see Fig. 2b). This maximum occurred near the SST front, indicated by the white arrow in Fig. 8. A subsurface maximum occurred north of the surface front near the middle of the Transect. Although there was little, if any, evidence of coastal upwelling off Ras Fartak, the spatial gradients in chlorophyll *a* and acoustic backscatter show strong gradients exist in plankton distributions near a surface temperature front.

3.4. ADCP backscatter distributions: Somalia

Between the evening of August 13 and mid-day on August 14, the *Baldrige* repeatedly crossed a cool surface filament that extended offshore from

the coastal upwelling center at Ras Hafun, Somalia (Fig. 1). The filament wrapped around the northern the edge of the Great Whirl where surface velocities exceeded 2 m s^{-1} (Fig. 1; Hitchcock et al., 2000). Transect T8 contains the ship's heading and the corresponding acoustic backscatter and surface properties in three consecutive sections that crossed the filament (Fig. 9). Surface temperature and salinity were variable across the 30 km width of the filament, with SST ranging from 22.5° in the filament center to $>26^{\circ}$ at the northern edge. Surface salinity similarly varied from 35.3 to 35.8 between the filament's center and its edge. These gradients in surface properties show the filament was derived from relatively fresh, cool surface waters in the upwelling zone.

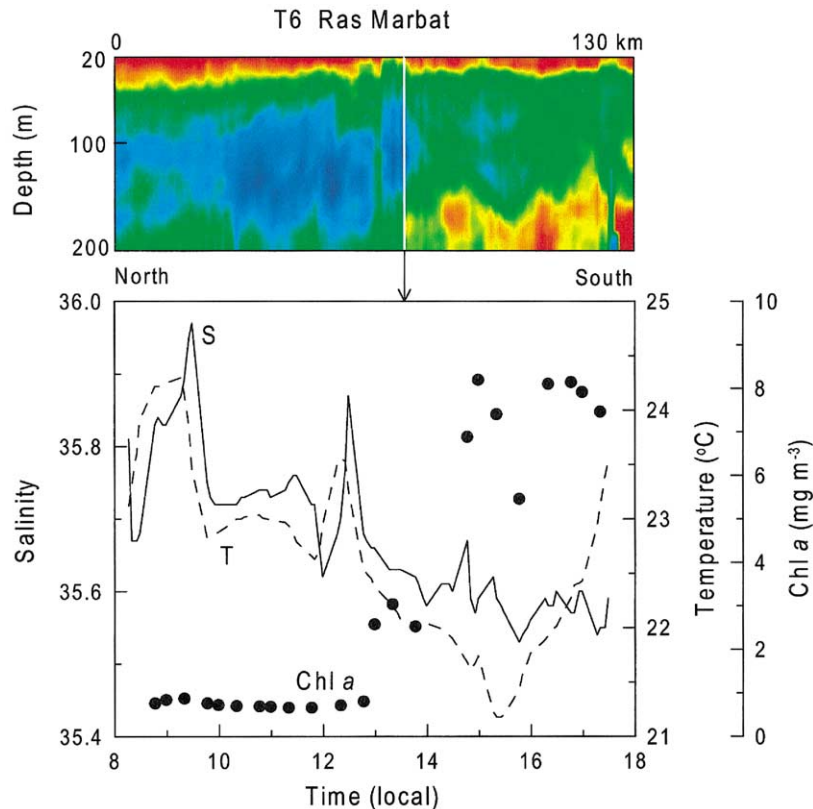


Fig. 7. Upper panel: the spatial distribution of acoustic backscatter intensity in the upper 20–200 m in Transect T6 in the coastal waters east of Ras Marbat, Oman. Color scale as in Fig. 3. The arrow in the ADCP backscatter plot shows where the increase in acoustic backscatter intensity corresponds to cooler, fresher surface waters with high chlorophyll *a* concentrations. Lower panel: corresponding surface salinity, temperature, and total chlorophyll *a* (Chl *a*) from the bow water intake at 3 m.

The ship left the filament at local noon and headed NE into warmer, saltier waters. The SST and surface salinity were rather uniform at 26°C and 35.7, respectively, as the ship began a 1500 km transect towards the ONR mooring in the central northern Arabian Sea (Fig. 9).

Spatial distributions of acoustic backscatter in T8 suggests a local maximum in zooplankton occurred in the upper 120 m of the cool filament. Zooplankton ADB in T8 varied from <10 to 40 g dw m⁻², with highest concentrations at the coolest SST of 23°C to 24°C (Fig. 10). Zooplankton ADB from August 12 are included in Fig. 10, corresponding to a period when the *Baldrige* was in recently upwelled waters at the eastern edge of the upwelling zone. Several unsuccessful MOC-

NESS tows were attempted in the upwelled waters on August 12, as described in Section 2.1. The ship spent considerable time on station and consequently no transect data are available from the upwelling zone. The zooplankton ADB from August 12 range from 1 to 30 g dw m⁻², while that in T8 vary from 4 to 40 g dw m⁻². The pattern of ADB in the recently upwelled waters and the filament is similar to that found off Ras Madrakah, Oman (compare Figs. 2 and 10) in that the zooplankton ADB-temperature relationship within the filament exhibits scatter, and frequently higher ADB, than that in recently upwelled waters. However, there appeared to be considerably more scatter in ADB within the Somali upwelling zone than in the Ras Madrakah upwelling area.

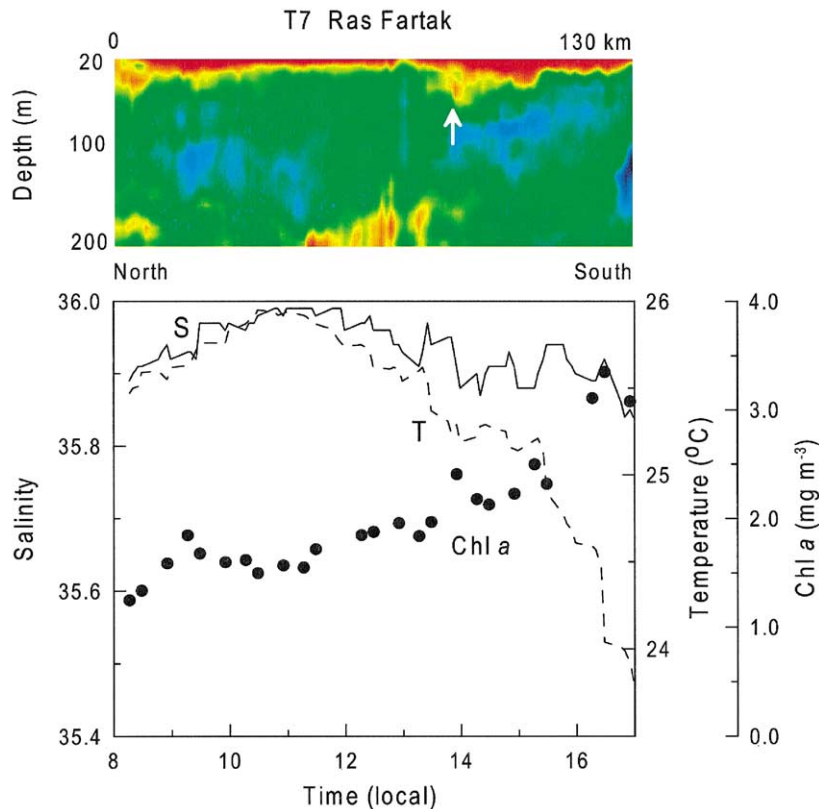


Fig. 8. Upper panel: the spatial distribution of acoustic backscatter intensity in the upper 20–200 m in Transect T7 in the coastal waters east of Ras Fartak, Yemen. Color scale as in Fig. 3. Lower panel: corresponding surface salinity, temperature, and total chlorophyll *a* (Chl *a*) from the bow water intake at 3 m.

The scatter in ADB in T8 reflects the repeated crossings of the ship into the feature and the warmer, saltier surrounding waters containing lower acoustic backscatter. Surface chlorophyll *a* concentrations, in contrast, varied only from 0.6 to 0.8 mg m⁻³ along Transect 8. Thus, surface pigment concentrations were less variable than zooplankton ADB off Somalia. Chlorophyll *a* concentrations increased to >0.8 mg m⁻³ as the ship left the filament and proceeded northeast.

4. Discussion

4.1. Mesozooplankton biomass

We used MOCNESS and Bongo net collections in addition to ADCP backscatter to evaluate

zooplankton biomass in the coastal upwelling zone and offshore waters, out to ca. 600 km, during the SW monsoon. Comparisons of biomass estimated from displacement volume measurements of net samples collected during GLOBEC cruise MB95-03 on the *Baldrige* and US JGOFS cruise TN050 on the R.V. *Thomas G. Thompson* (Smith et al., 1998b) allowed us to relate our near-shore observations to offshore biomass trends. Integrated biomass estimates from MOCNESS collections at stations M42 and M43 on the GLOBEC cruise, and S2 and S4 on the US JGOFS cruise suggested an increase in biomass seaward of the Omani upwelling zone (Table 2). Zooplankton sampling methods were similar on these two cruises, both utilizing MOCNESS nets with 1 m² net mouth area and 153 μm mesh to sample depth strata in daytime and night-time

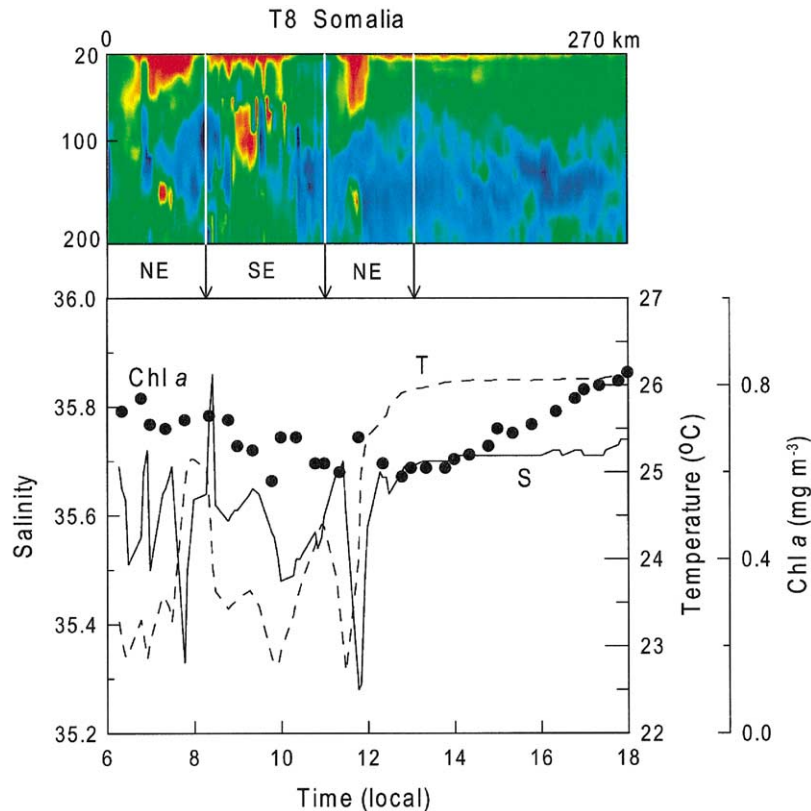


Fig. 9. Upper panel: the spatial distribution of acoustic backscatter intensity in the upper 20–200 m in Transect T8 at the northern perimeter of the Great Whirl. Color scale as in Fig. 3. Arrows in the ADCP backscatter plot indicate that the highest acoustic backscatter corresponds to relatively cool fresh surface waters at the eddy perimeter. The ship heading is designated as northeast (NE) or southeast (SE) in three consecutive crossings. Lower panel: corresponding surface salinity, temperature, and total chlorophyll *a* (Chl *a*) from the bow water intake at 3 m.

tows. We have included the Bongo tow data from the US JGOFS cruise (Table 2) because these are the only data available for the most inshore station sampled (Fig. 1).

Because integrated sample depths varied between station locations and between cruises, we further compared biomass estimates on a per unit volume basis (biomass m^{-3}). In general, zooplankton biomass derived from MOCNESS tows on the *Baldrige* in Omani coastal waters during August was lower than that at US JGOFS stations (Table 2). Both *Baldrige* and US JGOFS net tows extended to depths of 200–300 m, and therefore included the principal fraction of zooplankton in the water column (see Fig. 2). The Bongo tow to 50 m at station S1 on the US JGOFS line where

sonic depth was ca. 85 m is an exception (Fig. 1). The estimated biomass at S1 was 118 mg dw m^{-3} (7 mM C m^{-3}), which reflects the influence of the shallow depth of this station. A large proportion of the zooplankton biomass found in the upper 300 m at other US JGOFS stations was concentrated in the upper 50 m (Smith et al., 1998b; Lane and Smith, 1997; Fig. 2). This observation is also reflected in the strong acoustic backscatter signal seen in the upper 50 m region in *Baldrige* section T-5, located about 10 km from station S1 (Fig. 6). Zooplankton biomass per unit volume over the upper 200–300 m water column ranged from ca. 22 to 50 mg dw m^{-3} ($0.7\text{--}1.7 \text{ mM C m}^{-3}$) in MOCNESS tows collected from the *Baldrige* (Table 2) compared with $40\text{--}58 \text{ mg dw m}^{-3}$

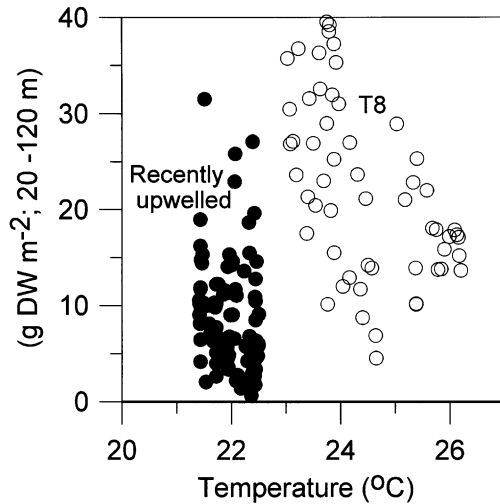


Fig. 10. (a) Acoustically determined biomass (ADB) for zooplankton in Somali coastal waters as a function of surface temperature on August 12, in the upwelling zone, and in Transect 8 on August 14. Transect 8 repeatedly crossed the cool filament at the northern perimeter of the Great Whirl (see Fig. 9).

($1.4\text{--}2\text{ mM C m}^{-3}$) at US JGOFS stations S2 and S4 located further offshore (Fig. 1; Table 2). Near the axis of the Findlater Jet at station S7, zooplankton biomass decreased to $12\text{--}21\text{ mg dw m}^{-3}$ ($0.4\text{--}0.7\text{ mM C m}^{-3}$).

The limited number of MOCNESS stations coupled with spatial and temporal variability, complicates any comparison of biomass indices from the two ships. However, estimates of zooplankton biomass per unit volume and depth-integrated biomass in Omani coastal waters (M42–M48) in early August were generally lower than those observed at US JGOFS stations during early September (S2–S4; 150–360 km offshore). To the extent that the data from the two ships can be compared, it would appear that zooplankton biomass increased between the coastal upwelling zone and surface waters 100–400 km offshore. Ashjian et al. (2002) reported a peak in acoustically estimated zooplankton biomass near US JGOFS station S3 (250 km offshore; Fig. 1). A potential explanation for the gradient of increased biomass offshore is provided in the following section (4.2), where we consider the potential role

of a filament in the export of zooplankton from an upwelling zone.

4.2. Mesozooplankton spatial distributions

Acoustic backscatter transects in Omani coastal waters show enhanced backscatter associated with surface fronts (e.g., Figs. 3, 6 and 8). The variability in backscatter typically occurred over tens of kilometers, a spatial scale typically observed for variability of physical properties and plankton distributions in coastal waters (Mackas et al., 1985). Zooplankton biomass maxima are often associated with fronts (e.g., Coyle and Hunt, 2000; Wade and Heywood, 2001), where physical processes such as convergence (Napp et al., 1996) and biological processes such as behavior, grazing and predation (Folt and Burns, 1999) contribute to patchiness in spatial distributions on the mesoscale.

The most extensive region of high backscatter intensity during the present study occurred in Transect 4 (T4) at the eastern edge of the coastal upwelling zone. Surface current vectors in T4 suggest this transect was near the origin of an upwelling filament. In two consecutive ADCP sections across the feature we estimate $\sim 300\text{ kg s}^{-1}$ of zooplankton ADB could potentially have been exported offshore from the upwelling zone. This export of zooplankton biomass is equivalent to an offshore flux of $25.9 \times 10^6\text{ kg dw day}^{-1}$. Since the ADB concentration of zooplankton within the upwelling zone is on the order of 15 g dw m^{-2} (see Fig. 3), then the filament could potentially export zooplankton out of an area of 1700 km^2 each day. The filament was about 60 km wide, so it could effectively ‘clear’ an area $30 \times 60\text{ km}^2$ each day, approximately the region bounded by Transects 4 and 5. If this estimate is typical of the magnitude of zooplankton export in upwelling filaments, these features may serve as the primary mechanism by which zooplankton associated with upwelling zones, such as the copepod *Calanoides carinatus*, are exported from the upwelling zone and transported offshore.

A second upwelling filament was surveyed in Transect 7 seaward of the coastal upwelling zone off Somalia. Here, the offshore zooplankton flux

in a daytime section was similar to T4, at 300 kg s^{-1} . This feature has previously been hypothesized as a mechanism for chlorophyll *a* and zooplankton export from the upwelling ‘wedge’ along the coast (Smith, 1984; Hitchcock et al., 2000). It differs from the Omani upwelling filaments in that it is narrower ($\sim 30 \text{ km}$), and peak current speeds reach 2 m s^{-1} (Fig. 1). Surface drifters deployed in the filament were carried east at $150\text{--}170 \text{ km day}^{-1}$ (Hitchcock et al., 2000). Given that zooplankton biomass near the origin of this feature is on the order of $10\text{--}20 \text{ g dw ADB m}^{-2}$, this filament contributes to offshore export of plankton biomass from the Somali coastal upwelling zone. The rapid export of zooplankton in this feature has been postulated as one explanation for relatively low concentrations of plankton biomass observed in the Somali upwelling zone (Bakun et al., 1998).

It is clear that cool filaments of recently upwelled water can potentially export large quantities of plankton biomass offshore. The cool subsurface waters that upwell near Ras Madrakah are advected offshore as filaments that follow ‘lows’ in sea surface topography (Brink et al., 1998; Manghnani et al., 1998). In the northern Arabian Sea, surface currents and sea surface height are dominated by the mesoscale eddy field (Flagg and Kim, 1998). The region of most intense filament generation is east of Ras Madrakah where a large eddy, centered near 17.5°N , 58.5°E , influenced sea surface topography throughout much of the SW monsoon in 1995 (Shi et al., 2000). The processes that generate cool filaments in the northern Arabian Sea may be similar to those in the California Current System (CCS; Strub et al., 1991; Fischer et al., 2002). Arabian Sea filaments are distinct, however, in that they extend longer distances offshore, and have higher inorganic nutrient concentrations and phytoplankton biomass than filaments in the CCS (Barber et al., 2001).

Sea-surface topography and satellite SST imagery from the SW monsoon indicate that offshore transport occurred in filaments as early as mid-June (Fischer et al., 2002). An upwelling filament surveyed east of Ras Madrakah with a SeaSoar, an undulating profiler, in late June contained high

concentrations of inorganic nutrients and chlorophyll *a* (Brink et al., 1998). Pigment signatures derived from high-performance liquid chromatographic analysis and size fractionated samples of pigments collected in a filament show that the autotrophic community is dominated by diatoms and other large phytoplankton (Latasa and Bidigare, 1998) typical of the upwelling zones. The sequence of US JGOFS cruises detected the presence of a filament on the southern station line from mid-July to mid-October (Barber et al., 2001). In mid-September the filament was sampled at S8, $\sim 720 \text{ km}$ offshore (Flagg and Kim, 1998), where primary productivity rates exceeded $200 \text{ mM C m}^{-2} \text{ day}^{-1}$ and chlorophyll *a* in the upper 50 m was $> 1.2 \text{ mg m}^{-3}$ (Barber et al., 2001).

Enhanced diatom biomass and high primary productivity rates in Arabian Sea filaments likely contribute to the maintenance of zooplankton as they are advected offshore from upwelling centers off Oman and Somalia. The ontogenetic life cycle of the ‘indicator’ copepod for upwelling in the northern Arabian Sea, *Calanoides carinatus*, illustrates how plankton organisms exploit the physical and biological characteristics of filaments. Reproduction in *C. carinatus* occurs in upwelling zones off Somali and Oman during the SW monsoon (Smith et al., 1998b). Adults of this species feed on large phytoplankton (Schnack, 1982; Smith, 1982), so the diatom-dominated phytoplankton community within filaments could sustain the large copepods as they are transported offshore. Based on Transect 4, the offshore advection of zooplankton in cool filaments is likely on the order of 50 km day^{-1} . At this rate, zooplankton could be transported to US JGOFS station S8 ($> 700 \text{ km}$ offshore) within two weeks. Clearly the physical and biological environment of cool filaments favor the occurrence of zooplankton such as *C. carinatus* in offshore waters.

Acknowledgements

We gratefully acknowledge the assistance of Shailer Cummings and Dave Forcucci throughout the study. Without the effort of the Captain and crew of the NOAA Ship *Malcolm Baldrige* this

project would not have been possible. Members of the GLOBEC scientific party, particularly Drs. L. Madin, P. Kremer, E. Clarke, and H. Verheye, made the cruise enjoyable. Mr. Leonard Hill (deceased) conducted the displacement volume analyses from samples collected on the NOAA Ship *Malcolm Baldrige*. This study was funded by awards from the Office of Naval Research (N00014-95-1-0252 to G. Hitchcock, N000149710156 to P. Ortner, and N00049510042 to S.L. Smith), and the National Science Foundation (Grant OCE 9310577 to S. Smith).

References

- Ahlstrom, E., Thraikill, J., 1963. Plankton volume loss with preservation. California Cooperative Fisheries Investigations, Report 9. California State Printing Office, Sacramento, CA, pp. 57–73.
- Ashjian, C.J., Davis, C.S., Gallagher, S.M., Alatalo, P., 2001. Distribution of plankton, particles, and hydrographic features across Georges Bank described using the video plankton recorder. *Deep-Sea Research II* 48, 245–282.
- Ashjian, C.J., Smith, S.L., Flagg, C.N., Idrisi, N., 2002. Distribution, annual cycle, and vertical migration of acoustically derived biomass in the Arabian Sea during 1994–1995. *Deep-Sea Research II* 49, 2377–2402.
- Baars, M.A., Osterhuis, S., 1997. Zooplankton biomass in the upper 200 m in and outside the seasonal upwelling areas of the western Arabian Sea. In: Pierrot-Bults, A.C., van der Spoel, S. (Eds.), *Pelagic Biogeography ICoPBII*. Proceedings of the Second International Conference. IOC/UNESCO, Paris, pp. 39–52.
- Bakun, A., Roy, C., Lluch-Cota, S., 1998. Coastal upwelling and other processes regulating ecosystem productivity and fish production in the western Indian Ocean. In: Sherman, K., Okemwa, E.N., Ntiba, M.J. (Eds.), *Large Marine Ecosystems of the Indian Ocean: Assessment, Sustainability, and Management*. Blackwell Scientific, Malden, MA, pp. 103–141.
- Barange, M., 1990. Vertical migration and habitat partitioning of six euphausiid species in the northern Benguela upwelling system. *Journal of Plankton Research* 12, 1223–1237.
- Barber, R.T., Marra, J., Bidigare, R.C., Codispoti, L.A., Halpern, D., Johnson, Z., Latasa, M., Goericke, R., Smith, S.L., 2001. Primary productivity and its regulation in the Arabian Sea in 1995. *Deep-Sea Research II* 48, 1127–1172.
- Brink, K., Arnone, R., Coble, P., Flagg, C., Jones, B., Kindle, J., Lee, C., Phinney, D., Wood, M., Yenstch, C., Young, D., 1998. Monsoons boost biological productivity in Arabian Sea. *EOS* 79, 168–169.
- Böhm, E., Morrison, J.M., Manghnani, V., Kim, H.-S., Flagg, C.N., 1999. The Ras al Hadd jet: remotely sensed and acoustic Doppler current profiler observations in 1994–1995. *Deep-Sea Research II* 46, 1531–1549.
- Boyd, C.M., Smith, S.L., 1983. Plankton, upwelling, and coastally trapped waves off Peru. *Deep-Sea Research I* 30, 723–742.
- Coyle, K.O., Hunt Jr, G.L., 2000. Seasonal differences in the distribution, density and scale of zooplankton patches in the upper mixed layer near the western Aleutian Islands. *Plankton Biology and Ecology* 47, 31–42.
- Coyle, K.O., Weingartner, T.J., Hunt Jr, G.L., 1998. Distribution of acoustically determined biomass and major zooplankton taxa in the upper mixed layer relative to water masses in the western Aleutian Islands. *Marine Ecology Progress Series* 165, 95–108.
- Currie, R.I., 1992. Circulation and upwelling off the coast of South-East Arabia. *Oceanologica Acta* 15, 43–60.
- Firing, E., Randa, J., Caldwell, P., 1995. Processing ADCP data with the CODAS Software System, Version 3.1. E. Firing ADCP Laboratory, JIMAR, University of Hawaii, 1000 Pope Rd., MSB 307, Honolulu, HI 96822, USA, unpublished manuscript.
- Fischer, A.S., Weller, R.A., Rudnick, D.L., Erickson, C.C., Lee, C.M., Brink, K.H., Fox, C.A., Leben, R.R., 2002. Mesoscale eddies, coastal upwelling, and the upper-ocean heat budget in the Arabian Sea. *Deep-Sea Research II* 49, 2231–2264.
- Flagg, C.N., Kim, H.-S., 1998. Upper ocean currents in the northern Arabian Sea from shipboard ADCP measurements collected during the 1994–1995 US JGOFS and ONR programs. *Deep-Sea Research II* 45, 1917–1959.
- Flagg, C., Smith, S.L., 1989. On the use of the acoustic Doppler current profiler to measure zooplankton abundance. *Deep-Sea Research I* 36, 455–474.
- Folt, C.L., Burns, C.W., 1999. Biological drivers of zooplankton patchiness. *Trends in Ecology and Evolution* 14, 300–305.
- GLOBEC, 1993. Implementation plan and workshop report for US GLOBEC studies in the Arabian Sea. US Global Ocean Ecosystem Dynamics Report No. 9, 105pp.
- Gjøsaeter, J., 1984. Mesopelagic fish, a large potential resource in the Arabian Sea. *Deep-Sea Research I* 31, 1019–1035.
- Heywood, K.J., 1996. Diel vertical migration of zooplankton in the Northeast Atlantic. *Journal of Plankton Research* 18, 163–184.
- Hitchcock, G.L., Key, E., Masters, J., 2000. The fate of upwelled waters in the Great Whirl, August, 1995. *Deep-Sea Research II* 47, 1605–1621.
- Holliday, D.V., Pieper, R.E., 1995. Bioacoustic oceanography at high frequencies. *ICES Journal of Marine Science* 52, 279–296.
- Ikedo, T., 1974. Nutritional ecology of marine zooplankton. *Memoirs of the Faculty of Fisheries, Hokkaido University* 22, 1–97.
- Lane, P., Smith, S., 1997. United States Joint Global Ocean Flux Study (US JGOFS) Technical Report: Zooplankton biomass in the upper water column of the Arabian Sea in 1994 and 1995. RSMAS Technical Report Number 97007, Miami, FL, 23pp.

- Latasa, M., Bidigare, R.R., 1998. A comparison of phytoplankton populations of the Arabian Sea during the Spring Intermonsoon and Southwest Monsoon of 1995 as described by HPLC-analyzed pigments. *Deep-Sea Research II* 45, 2133–2170.
- Lee, C.M., Jones, B.H., Brink, K.H., Fischer, A.S., 2000. The upper-ocean response to monsoonal forcing in the Arabian Sea: seasonal and spatial variability. *Deep-Sea Research II* 47, 1177–1226.
- Luo, J., Ortner, P.B., Forcucci, D., Cummings, S.R., 2000. Diel vertical migration of zooplankton and mesopelagic fish in the Arabian Sea. *Deep-Sea Research II* 47, 1451–1473.
- Mackas, D.L., Denman, K.L., Abbott, M.R., 1985. Plankton patchiness: biology in the physical vernacular. *Bulletin of Marine Science* 37, 652–674.
- Manghnani, V., Morrison, J.M., Hopkins, T.S., Böhm, E., 1998. Advection of upwelled waters in the form of plumes off Oman during the southwest monsoon. *Deep-Sea Research II* 45, 2027–2052.
- Morrison, J.M., Codispoti, L.A., Gaurin, S., Jones, B., Manghnani, V., Zheng, Z., 1998. Seasonal variation of hydrographic and nutrient fields during the US JGOFS Arabian Sea process study. *Deep-Sea Research II* 45, 2053–2101.
- Müller-Karger, F.E., Richardson, F.P., McGillicuddy, D., 1995. On the offshore dispersal of the Amazon's plume in the North Atlantic. *Deep-Sea Research I* 42, 2127–2137.
- Napp, J., Incze, L.S., Ortner, P.B., Siefert, D.L.W., Britt, L., 1996. The plankton of Shelikof Strait, Alaska: standing stock, production, mesoscale variability and their relevance to larval fish survival. *Fisheries Oceanography* 5, 19–38.
- Nordhausen, W., 1994. Distribution and diel migration of the euphausiid *Thysanoessa macrura* in Gerlache Strait, Antarctica. *Polar Biology* 14, 219–229.
- Powell, T.M., 1995. Physical and biological scales of variability in lakes, estuaries and the coastal ocean. In: Powell, T.M., Steele, J.H. (Eds.), *Ecological Time Series*. Chapman and Hall, New York, pp. 117–138.
- Roman, M., Smith, S., Wishner, K., Zhang, X., Gowing, M., 2000. Mesozooplankton production and grazing in the Arabian Sea. *Deep-Sea Research II* 47, 1423–1450.
- Schnack, S., 1982. Feeding habits of *Calanoides carinatus* (Krøyer) in the upwelling area off northwest Africa. *Rapports et proces-verbaux des reunions, Conseil permanent international pour l'exploration de la Mer* 180, 303–306.
- Schott, F., 1983. Monsoon response of the Somali current and associated upwelling. *Progress in Oceanography* 12, 357–381.
- Shi, W., Morrison, J.M., Böhm, E., Manghnani, V., 2000. The Oman upwelling zone during 1993, 1994 and 1995. *Deep-Sea Research II* 47, 1227–1247.
- Smith, S.L., 1982. The northwestern Indian Ocean during the monsoon of 1979: distribution, abundance and feeding of zooplankton. *Deep-Sea Research I* 29, 1331–1353.
- Smith, S.L., 1984. Biological indications of active upwelling in the northwest Indian Ocean in 1964 and 1979, and a comparison with Peru and northwest Africa. *Deep-Sea Research I* 31, 951–967.
- Smith, S.L., 1991. Growth, development and distribution of the euphausiids *Thysanoessa raschi* (M. Sars) and *Thysanoessa inermis* (Krøyer) in the southeastern Bering Sea. *Polar Research* 10, 461–478.
- Smith, S.L., 1992. Secondary production in waters influenced by upwelling off the coast of Somalia. In: Desai, B. (Ed.), *Oceanography of the Indian Ocean*. Oxford & IBH, New Delhi, pp. 191–199.
- Smith, S.L., Codispoti, L.A., 1980. Southwest monsoon of 1979: chemical and biological response of Somali coastal waters. *Science* 209, 569–600.
- Smith, S.L., Pieper, R.E., Moore, M.V., Rudstam, L.G., Greene, C.H., Zamon, J.E., Flagg, C.N., Williamson, C.E., 1992. Acoustic techniques for the in situ observation of zooplankton. *Ergebnisse der Limnologie* 36, 23–43.
- Smith, S.L., Codispoti, L.A., Morrison, J.M., Barber, R.T., 1998a. The 1994–1996 Arabian Sea expedition: an integrated, interdisciplinary investigation of the response of the northwestern Indian Ocean to monsoonal forcing. *Deep-Sea Research II* 45, 1905–1915.
- Smith, S., Roman, M., Prusova, I., Wishner, K., Gowing, M., Codispoti, L.A., Barber, R., Marra, J., Flagg, C., 1998b. Seasonal response of zooplankton to monsoonal reversals in the Arabian Sea. *Deep-Sea Research II* 45, 2369–2403.
- Stanton, T.K., Wiebe, P.H., Chiu, D., Benfield, M., Scanlon, L., Martin, L., Eastwood, R.L., 1994. On acoustic estimates of zooplankton biomass. *ICES Journal of Marine Science* 51, 505–512.
- Strub, T., Kosro, P.M., Huyer, A., 1991. The nature of the cold filaments in the California current system. *Journal of Geophysical Research* 96, 14743–14768.
- Van Couwelaar, M., Angel, M.V., Madin, L.P., 1997. The distribution and biology of the swimming crab *Charybdis smithii* McLeay, 1838 (Crustacea: Brachyura: Portunidae). *Deep-Sea Research II* 44, 1251–1280.
- Verheye, H.M., Hutchings, L., Huggett, J.A., Painting, S.J., 1992. Mesozooplankton dynamics in the Benguela ecosystem, with emphasis on the herbivorous copepods. *South African Journal of Marine Science* 12, 561–584.
- Wade, I.P., Heywood, K.J., 2001. Acoustic backscatter observations of zooplankton abundance and behaviour and the influence of oceanic fronts in the northeast Atlantic. *Deep-Sea Research II* 48, 899–924.
- Watkins, J.L., Morris, D.J., Ricketts, C., 1985. Nocturnal changes in the mean length of a euphausiid population: vertical migration, net avoidance, or experimental error? *Marine Biology* 86, 123–127.
- Wiebe, P., 1988. Functional regression equations for zooplankton displacement volume, wet weight, dry weight, and carbon: a correction. *Fishery Bulletin* 86, 833–835.
- Wiebe, P.H., Burt, K.H., Boyd, S.H., Morton, A.W., 1976. A multiple opening/closing net and environmental sensing

- system for sampling zooplankton. *Journal of Marine Research* 34, 341–354.
- Wiebe, P.H., Boyd, S.H., Davis, B.M., Cox, J.L., 1982. Avoidance of towed nets by the euphausiid *Nematoscelis megalops*. *Fisheries Bulletin* 80, 75–81.
- Wishner, K.F., Gowing, M.M., Gelfman, C., 1998. Mesozooplankton biomass in the upper 1000 m in the Arabian Sea: overall seasonal response and geographic patterns, and relationship to oxygen gradients. *Deep-Sea Research II* 45, 2405–2432.
- Zhou, M., Nordhausen, W., Huntley, M., 1994. ADCP measurements of the distribution and abundance of euphausiids near the Antarctic Peninsula in winter. *Deep-Sea Research I* 41, 1425–1445.